



SPE 80921

Analysis of Experimental Data of ESP Performance Under Two-Phase Flow Conditions

Raghavan Beltur and Mauricio Prado, SPE, The University of Tulsa, Javier Duran, SPE, Ecopetrol, Rui Pessoa, SPE, PDVSA-Intevep.

Copyright 2003, Society of Petroleum Engineers Inc.

This paper was prepared for presentation at the SPE Production and Operations Symposium held in Oklahoma City, Oklahoma, U.S.A., 22–25 March 2003.

This paper was selected for presentation by an SPE Program Committee following review of information contained in an abstract submitted by the author(s). Contents of the paper, as presented, have not been reviewed by the Society of Petroleum Engineers and are subject to correction by the author(s). The material, as presented, does not necessarily reflect any position of the Society of Petroleum Engineers, its officers, or members. Papers presented at SPE meetings are subject to publication review by Editorial Committees of the Society of Petroleum Engineers. Electronic reproduction, distribution, or storage of any part of this paper for commercial purposes without the written consent of the Society of Petroleum Engineers is prohibited. Permission to reproduce in print is restricted to an abstract of not more than 300 words; illustrations may not be copied. The abstract must contain conspicuous acknowledgment of where and by whom the paper was presented. Write Librarian, SPE, P.O. Box 833836, Richardson, TX 75083-3836 U.S.A., fax 01-972-952-9435.

Abstract

Electrical Submersible Pumps (ESP's) are well known to have a good predictable performance for single phase, low viscosity liquids. In the oil industry, oil production is associated with the production of gas. The presence of gas deteriorates the performance of the pump. The performance deterioration varies with the amount of gas and the intake pressure at which the pump is operated. So far no good predictive method is available to predict the performance of the ESP under two-phase conditions. Presently the industry is using the homogeneous model, correlations and other models to predict this performance. In the homogeneous model the two-phase flow head is assumed to be the same as single-phase head (provided by the manufacturer) at a total mixture flow rate. The available correlations are specific to the tested type of pump and to the tested number of stages. Finally to predict performance on model, no general model has been developed to predict two-phase performance of the ESP due to complexity of two-phase flow, pump geometry and speed at which it is operated. Researchers, Lea and Bearden (1982), Cirilo (1998), Romero (1999) and Pessoa (2000) have concluded through experimental results that the application of the homogeneous model gives good prediction only at low gas fractions (in the order of 2 to 5 %) at the intake. At higher gas fraction the experimental results shows that performance is well away from the homogeneous model predicted performance.

The University of Tulsa Artificial Lift Projects – TUALP is currently conducting experimental and theoretical research on the two-phase behavior of electrical submersible centrifugal pumps, using a 22-stage Mixed flow type, series 513 pump with best efficiency flow rate of 6100 BPD to gather data on stage wise performance under two-phase flow conditions. Air and water were used as working fluids. This is a unique

facility that has pressure gauges fitted across each stage. It not only helps to study the stage wise behavior but also the effect of number of stages on cumulative performance of pump under two-phase flow conditions. This paper focuses on analysis of data collected at TUALP facility.

Introduction

Centrifugal pumps are dynamic single or multistage devices that use kinetic energy to increase liquid pressure. To handle low viscosity, single-phase incompressible fluids, existing impeller and diffuser designs are very successful, but are severely impacted by free gas, highly compressible or viscous fluids.

The relationship between the head developed by the pump and the flow rate through the pump for a certain rotational speed is determined by a specific single-phase performance curve, which is experimentally determined using water as the working fluid.

The head performance curves are valid then for any other low viscosity single-phase liquid, independent of its density. Brake horsepower and efficiency curves are usually presented on the same chart. The performance of multistage pumps handling incompressible fluids is presented on average per stage. An example of these performance curves is shown in Figure 1.

Two vertical lines define the lower and upper limit where it is recommended to operate the equipment. The best efficiency point is the point of maximum efficiency within the operating range, and is usually abbreviated as BEP.

For low viscosity oil with no free gas or very low volumetric free gas fractions (< 2%) at pump intake condition, the sizing of a multi-stage ESP has shown good agreement based on the water performance curves supplied by the manufacturer, corrected by the homogeneous model approach.

While handling higher contents of free gas, the centrifugal pump suffers head degradation. Performance prediction based on single-phase water performance curves corrected by the homogeneous model cannot be used. In addition to performance degradation while handling free gas, submersible pumps also require prediction of surging and gas lock conditions. The homogeneous model is incapable of correctly addressing those problems.

Surging is a phenomenon related to instability of the pump performance. Though fluctuation is observed in an entire range of liquid flow rates in two-phase flow, it is more severe at low liquid flow rates, especially to the left of the best efficiency point. It is also known in literature as heading. The term instability is also used in the technical literature in reference to this phenomenon. Studies from the nuclear industry state that surging appears as a discontinuity in the head performance, and such discontinuity is a consequence of a change in flow pattern from dispersed bubble or turbulent churned flow to stratified or slug flow. This abrupt fluctuation in performance is observed for flow rates smaller than the best efficiency point and changes with the amount of gas at the pump intake. An example of the pressure fluctuation during surging, with respect to time, is shown in Figure 2.

Gas lock is the next deteriorating stage after surging. During gas lock conditions, the pump stops delivering head. Once the pump is gas locked, it could be brought to normal operating condition by either increasing the intake pressure or stopping the pump so that gas is pushed out of suction by liquid.

A comparison between the experimentally determined head performance for the pump used in this study and the predicted performance, using the homogeneous model, is shown in Fig 3. One can see that the actual two-phase flow performance is considerably different from the single-phase performance and from the homogenous model. In order to correctly design, analyze and troubleshoot ESP applications in gassy environments, the performance of ESP under multiphase conditions must be known. Additionally, extensive theoretical and experimental research must be conducted to better understand this complex phenomenon.

Homogeneous Method For ESP Multiphase Performance

The traditional method of predicting the two-phase performance of an ESP pump is based on the homogeneous model. In this model, the two-phase mixture is assumed to behave as a homogeneous fluid. The two-phase head is then assumed equal to the single-phase performance head at the total in situ mixture flow rate. The total mixture flow rate q_m is the sum of the in situ liquid q_l and gas flow rates q_g , and is expressed as:

$$q_m = q_l + q_g \quad (1)$$

Considering these assumptions, the two-phase stage head H_{tp}^{stage} can be expressed as:

$$H_{tp}^{stage} = H_{sp}^{stage} \{q_m\} \quad (2)$$

where $H_{sp}^{stage} \{q_m\}$ is the single-phase head as a function of mixture flow rate q_m .

Similarly, the two-phase stage pressure increment ΔP_{stage}^{tp} can be written as:

$$\Delta P_{stage}^{tp} = H_{sp}^{stage} \{q_m\} g \rho_m^{no\ slip} \quad (3)$$

The mixture density is equal to the no-slip mixture density $\rho_m^{no\ slip}$, and is expressed as:

$$\rho_m^{no\ slip} = (1 - \lambda_g) \rho_l + \lambda_g \rho_g \quad (4)$$

where λ_g is the insitu no-slip gas fraction, ρ_g and ρ_l are insitu gas and liquid densities respectively.

The two-phase head performance based on water density can be expressed as a function of gas fraction, fluid densities and liquid flow rate as shown below:

$$H_{tp}^{water} = \left[(1 - \lambda_g) + \frac{\lambda_g \rho_g}{\rho_w} \right] H_{sp}^{stage} \{q_m\} \quad (5)$$

The traditional way of head prediction based on the homogeneous model provides a good approximation, when the mixture is homogeneous inside the pump. Homogeneous flow can occur only at low gas void fractions. The effect of two-phase flow results in some head degradation at higher void fractions. The homogeneous model predicts the head performance across all ranges of liquid flow rates and does not account correctly for surging and gas locking phenomena.

A comparison of homogenous models which can be developed based on actual recorded pressures at each stage and theoretical model developed based on homogenous pressures stagewise taking pump intake pressure as the base is shown in Figure 3. The actual performance is poorer than predicted by both models. The error at high liquid flow rates is less, compared to the error predicted at low liquid flow rates. At high liquid flow rate the mixture is more or less homogeneous with finely dispersed bubble and as the liquid flow rate reduces the flow pattern changes towards slug and churn flow.

Literature Review

Regarding the ESP performance under two-phase flow condition, very few studies are available. The isolated experiments conducted so far have been fundamental to understand trends and to provide insight on real behavior of ESP's when handling multiphase flow.

The nuclear industry, which has done extensive study, has few models that unfortunately cannot be used by the petroleum industry as the pumps used by the nuclear industry are of different design and of large diameter.

The petroleum industry is mainly concerned with multi-stage small diameter pumps (Electric Submersible Pumps) at higher intake pressures and gas fraction, whereas the nuclear industry focuses on single-stage, very low intake pressures and low void fraction.

Most of the petroleum industry research has been of an empirical nature, due to the complexity of the phenomena that rule centrifugal pump behavior.

Dunbar

Dunbar (1989) presented a general correlation for application of homogeneous model in a graphical form. The author relates the maximum gas liquid ratio where homogeneous model can be applied as a function of stage intake pressure. Dunbar constructed a reference curve called “Dunbar Curve” for minimum intake pressure that should be attained for a given gas liquid ratio, to apply homogeneous model or to account for no head degradation. Unfortunately his work does not provide information on theoretical aspects.

Lea and Bearden

Lea and Bearden (1982) tested three different pumps, the I-42B and C-72 of radial type stages and the K-70, which is of, mixed flow type, using diesel-CO₂ as two-phase mixture. Experiments were conducted to observe the behavior of ESP under two-phase flow conditions. This was essentially an experimental work and the authors presented no correlations or models to account for the observations.

Turpin

Turpin (1986) using the data of Lea and Bearden, developed empirical correlations to predict the head-capacity curve for the studied pumps as a function of the free gas-liquid ratio, liquid flow rate and pump intake pressure. Two correlations to predict two-phase head performance were achieved. One single correlation for I-42B radial and K-70 Mixed type Pump and another for C-72 radial Pump. These Correlations are pump specific and can predict the head capacity curve fairly well for low gas volumes at low intake pressures and for higher gas volumes at higher suction pressures. The prediction falls off in the direction of higher gas and lower pressure conditions, however the region of poor predictive capability of these correlations coincides with the region of unacceptable pump performance.

Cirilo

Cirilo (1998) measured the performance of three different submersible centrifugal pumps for handling two-phase flow. Two pumps were of mixed flow type (GN4000 and GN7000), and another one was radial type (GN2100). The experimental data were obtained using air and water as working fluids. The effect of number of stages were studied with 6,12 and 18 stages using GN4000 pump.

An important contribution of this work was a simple correlation to determine the maximum free gas fraction (λ_g) for stable operation of tested mixed flow electric submersible pumps.

$$\lambda_g = 0.0187 P_i^{0.4342} \quad (6)$$

where P_i is the pump intake pressure in psia.

Pessoa

Pessoa (1999) performed some tests with a tapered pump composed by a 104-stage GC4100 pump (mixed flow) and a 20-stage GCNPSH pump (highly axial flow). Real crude and gas were used as fluids at the PDV-INTEVEP experimental well. Both single-phase and two-phase tests were done with light (32.5 °API) and heavy (11.6°API) crude oil with a 0.7 specific gravity natural gas. The pump intake pressure was analyzed in the range between 150 and 400 psia.

Romero

Romero (1999) evaluated an improved model of stage with slotted impeller named Advanced Gas Handler (AGH), designed to increase the maximum free gas fraction that electric submersible pumping systems can handle. She used Cirilo's experimental data for a 12-stage GN4000 pump (mixed flow) in order to establish a comparative base scenario without AGH. Correlations were developed to predict two-phase head performance for the pump GN4000 and the tested Advanced Gas Handler on dimensionless parameters.

Sachdeva

Sachdeva (1989) presented the first comprehensive model developed in the petroleum industry. His work was an adaptation of the nuclear industry models to the multi-stage pumps used on ESP. This work was not experimental in nature but included data from Lea and Bearden (1982) to calibrate the model and to develop a correlation for the two-phase flow head.

Pessoa

Pessoa (2000), conducted experiments at state of art facility provided at TUALP using Air-Water at 100 psig intake pressure keeping gas mass flow rate constant and varying only liquid flow rate. This experimental set up has a pump with 22-stages with facility to measure pressure across each stage. For the first time stage wise two-phase performance were evaluated and presented experimental results on the basis of average efficiency of the pump and average BHP consumption. Calculation of input BHP was based on measured torque and pump shaft rpm.

Experimental Research at TUALP

In 2000, Pessoa used a, 22-stage mixed type pump (series 513,BEP 6100 BPD), modified to measure the pressure at each individual stage. The experimental setup is shown in Figure 4. This facility was further modified by Beltur (2002) with electro-pneumatic flow control valves to control automatically the intake pressure, liquid and gas flow rate. These valves were interfaced with computer using for automatic control.

Temperature transmitters were used to measure temperatures only at the inlet and the discharge points and the liquid and gas flow rates were measured using mass flow meters.

Selecting air-water as the test fluid has certain advantages. The solubility of air with water is negligible. With the familiar

knowledge of the physical properties of both fluids, it is possible to determine exact physical properties across each stage. With air-water as the testing fluid, the pump faces the worst condition in two-phase flow, as the separation of air with water is very fast, compared to oil and gas.

Single Phase Tests

Single-phase tests were conducted to compare the performance with the manufacturer-supplied curve. These tests were conducted at 50 Hz at intake pressures 100, 150, 200 and 250 psig to check the repeatability of single-phase performance. Reasonable repeatability was observed. An example showing the stage-wise pressure increment for single-phase at the pump intake pressure of 100-psi is shown in Figure 5. It can be seen from the Figure 5, that each stage performance is different and just considering one average pump performance for analysis will not be a good approach. For comparison, stage-wise performance fits were generated. Based on data collected at four different intake pressures, trend line curves were defined for single-phase stage-wise performance. As an example, single-phase performance of the 10th stage with the polynomial fit is shown in Figure 6.

As each stage performance is different on actual liquid flow rates, a new approach based on dimensionless flow rates and dimensionless pressure increments was considered.

The dimensionless pressure increment is expressed as a ratio of pressure increment to shut in pressure increment. Shut in pressure increment is the pressure increment recorded at zero liquid flow rate.

$$\Delta P_{n \text{ Stage}}^d = \frac{\Delta P_{n \text{ stage}}}{\Delta P_{n \text{ Stage shutin}}^{sp}} \quad (7)$$

Similarly, the dimensionless flow rate is expressed as the ratio of liquid flow rate to maximum single-phase liquid flow rate at which no performance is observed and is given as:

$$q_{l \text{ n Stage}}^d = \frac{q_l}{q_{l \text{ n Stage}}^{sp \text{ max}}} \quad (8)$$

Both the maximum single-phase liquid flow rate and shut in pressure increment were calculated based on performance polynomial fits of the stages. It can be seen from dimensionless plot shown in Figure 7 that, except for the first stage, all other stages fall in the same narrow range.

Analysis of Two-Phase Data

Two-phase data were collected, keeping pump speed constant at 2916 RPM (50 HZ) at intake pressure from 50 psig to 250 psig in steps of 50-psig increments. For a set of data, maintaining constant pump intake pressure and gas flow rate, only liquid flow rate was varied from maximum flow rate to minimum possible or zero liquid flow rate. Total number of data points collected on two-phase tests is 1944.

Two-Phase Performance

An example of stage-wise performance for a gas rate of 30000 Scfd at different intake pressure is shown in Figure 8. Stage-wise two-phase pressure increment performance shows that each stage has a different performance. Performance of the initial stages is very poor compared to the performance of downstream stages. The result of 100-psig-intake pressure shows very poor performance in the first two stages, as the mixture flow is not homogeneous and the stage intake gas fraction is high. As the mixture moves progressively to the downstream stages, the mixture gets more homogeneous due to turbulence generated by the speed of the impeller, and the gas fraction reduces due to increment in pressure in each stage. This promotes better intake conditions towards downstream stages resulting in better performance towards down stream stages. From Figure 8, it can also be observed that with the increase in the intake pressure, the liquid flow rate, at which maximum pressure increment is developed, moves towards a lower flow rate. I.e. with the increase in pump intake pressure, the operable range of liquid flow rate increases.

As the liquid flow rate reduces, the pressure increment increases to a certain value of liquid flow rate, at which stage shows peak performance. To the left of this peak performance liquid flow rate, the two-phase performance of the stages drops with a steep positive slope. This sudden drop in performance can be attributed to a change in the flow regime from bubbly flow to slug flow. As the liquid flow rate is reduced further, recovery in pump performance is observed. This recovery may be due to the homogeneous nature of a mixture with higher mixture density than gas, as the flow regime may be in annular or mist flow.

As seen earlier, the dimensionless single-phase performance for all stages falls in a narrow range. An example of dimensionless plot of two-phase flow is shown in Figure 9 for a gas flow rate of 30000 Scfd and at different intake pressures.

To calculate two-phase dimensionless data, the maximum pressure is taken as shut in single-phase pressure increment $\Delta P_{n \text{ Stage shutin}}^{sp}$ and maximum single-phase flow rate $q_{l \text{ n Stage}}^{sp \text{ max}}$ is taken as flow rate at which the pressure increment is zero.

Stage dimensionless pressure increment is given as:

$$\Delta P_{n \text{ Stage}}^d = \frac{\Delta P_{n \text{ stage}}^{tp}}{\Delta P_{n \text{ Stage shutin}}^{sp}} \quad (9)$$

Similarly, the stage dimensionless liquid flow rate is given as:

$$q_{l \text{ n Stage}}^d = \frac{q_l}{q_{l \text{ n Stage}}^{sp \text{ max}}} \quad (10)$$

It can be seen in Figure 9, at 100-psig-pump intake pressure stage performances are different even on dimensionless parameters at all liquid flow rates. As the intake pressure is

increased, it can be seen at higher liquid flow rate that the dimensionless performance falls in narrow range as in the case of single-phase tests. In addition, with the increase in intake pressure the point of peak performance liquid flow rate moves to lower liquid flow rate.

Pressure Degradation

In order to check for the trend in pressure increment degradation with respect to the single-phase and homogeneous model, data of pressure degradation were plotted against dimensionless liquid flow rate.

Pressure degradation, with respect to single phase D_p^{sp} , is the difference between the pressure increments for the considered liquid flow, based on the single-phase performance trend line and actual pressure increment in two-phase flow condition at the same liquid flow rate.

$$D_p^{sp} = \Delta P^{sp} - \Delta P^{tp} \quad (11)$$

Similarly, pressure degradation on the homogeneous model, D_p^{hom} , is the difference between the homogeneous pressure increments at total mixture flow rate on single-phase performance trend line and actual pressure increment in two-phase flow condition at the same liquid flow rate.

$$D_p^{hom} = \Delta P^{hom} - \Delta P^{tp} \quad (12)$$

The plot of degradation on a stage-wise basis, with respect to single-phase and homogeneous model is shown in Figures 10 and 11, respectively. The stage position has an important effect on degradation. From Figure 10, it can be seen that the downstream stages show less degradation compared to the upstream stages.

While comparing stage degradation with the homogeneous model shown in Figure 11, it can be seen that downstream stages at certain liquid flow rates show very small degradation. Higher degradation with respect to the homogeneous model is observed to the left and right of this flow rate. This shows that the homogeneous model can be applied only after a certain number of stages, and works only at a certain liquid flow rate.

An example of the effect of stage position is shown in Figure 12 for the test conducted at 50 psig. The plot shows that downstream stages perform much better and the range of liquid flow rate where the pump can be operated successfully increases with the number of stages.

The performance of the pump and the effect of intake pressure are of paramount importance. The amount of gas handled by the pump increases with the intake pressure. Comparing the results at 50 psig, shown in Figure 12, with the results at 200 psig intake pressure, shown in Figure 13, it can be seen that at 50 psig intake pressure, the pump almost stops performing beyond 12500 SCFD, where as at 200 psig intake pressure pump could handle upto 65000 SCFD of gas flow rate.

The effect of pump intake pressure was studied and an example for the 16th stage at different gas flow rates is shown in Figure 14. It can be seen again here that for a considered gas flow rate with the increase in intake pressure, stage performance improves and peak performance liquid flow rate moves to a lower liquid flow rate. It is interesting to note that at certain liquid flow rates, the two-phase performance is almost the same at different pressures.

As the test facility has the pressure gauges mounted on each stage, it was possible to study the effect of number of stages on average pump performance. The Figure 15 shows the average stage pressure increment for the gas flow rate of 30000 scfd at different intake pressures. It can be seen here that with the increase in number of stages the average stage performance of pump increases. Also with the increase in number of stages the liquid flow rate at which peak performance is observed also moves towards left to lower liquid flow rate.

Since the stage number has important effect on average performance of the pump, any correlation developed on average performance may lead to erroneous prediction. Further analysis was made only on stage wise.

The effect of gas fraction on degradation at the intake of each stage was studied. The Figure 16 and 17 shows the degradation trend with respect to single phase and homogeneous model for stage 16 at the pump intake pressure of 250 psig and at different gas flow rates. It can be seen here degradation shows definite trend with the gas fraction. Only at the very low gas fraction the plot shows degradation with very high slopes (almost vertical). This region falls in the liquid flow rate beyond the maximum capacity of the stage at which negative pressure increment is observed for the considered gas flow rate. For future analysis the data containing negative pressure increments are neglected.

A plot of degradation with respect to single phase as a function of gas fraction at the intake of each stage is shown in Figure 18. Here the first stage and second stage data were neglected as it is seen the performance of these stages are poor, unpredictable and most of the energy is spent on homogenizing the mixture. It can be seen in Figure 18 that degradation curves over laps for all stages, showing a considerably thick band on degradation across gas fraction. This indicates that apart from the gas fraction at the stage intake other variables like liquid flow rate, gas rate and intake pressure has influences on the pump performance.

The plots of degradation with respect to single-phase performance against gas fraction as a function of liquid flow rate, insitu gas rate and pump intake pressure shown in Figures 19, 20 and 21 respectively. In all these plots no clear trend is observed with respect to variables considered to establish correlation.

In order to see the pressure effect, new term Homogenous Dimensionless Pressure Increment was considered. The

Homogenous dimensionless pressure increment ΔP_{Hom}^d is given as the ratio of actual pressure increment with respect to the Homogeneous Shut in Pressure Increment.

$$\Delta P_{Hom}^d = \frac{\Delta P^{tp}}{\Delta P_{Shutin}^{d.hom}} \quad (13)$$

The shut in homogenous Pressure Increment $\Delta P_{Shutin}^{D.Hom}$ is expressed as:

$$\Delta P_{Shutin}^{d.hom} = \Delta P_{shutin}^{sp} * \frac{\rho_m}{\rho_w} \quad (14)$$

where ΔP^{tp} is the recorded two-phase pressure increment, ΔP_{shutin}^{SP} is the shut in single-phase pressure increment, ρ_w is the density of water, ρ_m is the insitu mixture density.

Here the effect of intake pressure is taken care off by the mixture density.

The other parameter dimensionless liquid flow rate is expressed as the ratio of actual liquid flow rate to the maximum single-phase liquid flow rate that the stage can handle and is expressed as in Equation 10.

The Dimensionless homogeneous pressure increment is plotted as function of dimensionless liquid flow rate for varying gas fraction is shown in Figure 22.

Here it can be seen that the plots shows clear trend with small band for each gas fraction. The data were segregated on insitu gas fraction and polynomial fit was developed for different gas fraction. The Figures 23-26 shows the plot for 1,3,7 and 9.25 % gas fraction respectively with trend fit curve. Beyond 7 % insitu gas fraction the data points at lower liquid flow rate shows wider spread and the performance curve shows deterioration to left of certain liquid flow with positive slope. Further as the liquid flow rate reduces recovery in performance is observed.

The sixth degree polynomial fit for stage homogeneous dimensionless pressure increment as a function of dimensionless liquid flow rate for different gas fraction is expressed as:

$$\Delta P_{hom}^d = \sum_{j=0}^6 C_j (q_l^d)^j \quad (15)$$

The plot based on above fit for different gas fraction is shown in Figure 27. Beyond 8 % gas fraction the homogeneous dimensionless performance fit curves shows some over lapping. This may be attributed to severe fluctuation or surging at these gas fractions.

Average Pump Efficiency and Average Brake Horse Power (BHP) comparisons were made to observe the behavior of these two parameters. Stage-wise efficiency could not be calculated, as it is difficult to know the BHP consumed by each stage, because it is known that each stage performance is different and intake condition and volumetric flow rate is different. Stage-wise hydraulic horsepower is calculated considering both isothermal and adiabatic compression of gas.

The raw data records the RPM and torque in pounds-inches. The BHP consumed by an average stage is calculated by:

$$BHP = rpm(\tau / 63025.36) \quad (16)$$

The efficiency η of the average pump is given as:

$$\eta = \frac{Hy.HP_{Liquid} + Hy.HP_{Gas}}{BHP} \quad (17)$$

Liquid hydraulic horsepower $Hy.H.P_L$ is given by:

$$Hy.H.P_{Liquid} = \Delta P * \frac{144}{60 * 550} * \frac{q_l * 5.614587}{24 * 60} \quad (18)$$

As the gas compression process is not clearly understood inside the stages, the gas hydraulic horsepower was calculated considering both the adiabatic and isothermal processes. On a stage-wise calculation, a very small difference was found between both assumptions, as pressure and temperature increment on each stage is small.

Gas hydraulic horsepower adiabatic $Hy.H.P_{g\text{ adiabatic}}$ is given by:

$$Hy.H.P_{g\text{ adiabatic}} = \frac{144}{60 * 550} * \frac{M_g}{24 * 60} * \frac{10.7316 * (T + 460)}{28.9700} * \left(\frac{P_2}{P_1} \right)^{\frac{K-1}{K}} * \frac{K}{K-1} \quad (19)$$

Gas hydraulic horsepower isothermal $Hy.H.P_{g\text{ isothermal}}$ is given by:

$$Hy.H.P_{g\text{ isothermal}} = \frac{144}{60 * 550} * \frac{M_g}{24 * 60} * \frac{10.7316 * (T + 460)}{28.9700} * LN \left(\frac{P_2}{P_1} \right) \quad (20)$$

A plot for efficiency based on adiabatic horsepower is shown in Figure 28. It can be seen here that with the increase in gas rate, the best efficiency point moves towards higher liquid flow rate.

A plot for comparison of average two-phase BHP consumption with respect to single-phase is shown in Figure 29. Here again, it can be observed with increase in gas flow rate that the BHP consumption decreases.

Conclusions

1. The petroleum industry lacks a general model to predict an ESP's performance under two-phase flow conditions.
2. Available correlations for predicting pump performance under two-phase flow conditions are limited and are based on average pump performance. Previous correlations are pump specific and limited to the number of stages used in the test setup.
3. The hydrodynamic conditions vary across each stage over the pump. This results in a variation in pump performance and also in horsepower consumption. Any prediction based on average performance may lead to erroneous results.
4. Dunbar (1989) developed a correlation for predicting the conditions where pump performance could be obtained using the homogeneous model. He also presented a procedure to account for head degradation when the homogeneous model cannot be applied. Critical parameters for application of this procedure were not presented.
5. From the experimental results of Cirilo (1998), it can be seen that for a constant gas fraction, the pump performance increases with increase in intake pressure until a critical pressure beyond which any increase in intake pressure will not result in improvement in pump performance. This can be compared with the region above the *ALIM* curve of Dunbar (1989).
6. Romero (1999) developed correlations for head performance and minimum liquid flow rate at which surging occurs as a function of gas void fraction. The applicability of the correlation was found to be limited to the pump with a specific number of stages and intake pressure was not considered.
7. The current TUALP research program has concluded single- and two-phase water-air stage-wise performance data for a 22-stage pump at an intake pressure of 100 psig at 55 Hz, and intake pressures of 100, 150, 200 and 250 psig at 50 Hz.
8. The average behavior of the pump is significantly different from the one observed for each stage.
9. The average best efficiency point in terms of liquid flow rate increases as gas flow rate increases.
10. The behavior of the pressure increment and total hydraulic horsepower is different for each of the stages.
11. Current knowledge is not sufficient to develop a general and accurate model for predicting head degradation, gas lock and surging conditions.
12. The performance data obtained in this work is limited to air-water mixtures.

Acknowledgements

The authors appreciate the technical and financial support of Tulsa University Artificial Lift Projects' member companies. The progress on this work is the result of the support of ENI - AGIP, CENTRILIFT, PDVSA, PEMEX, ONGC, SCHLUMBERGER, SHELL and TOTALFINA ELF.

Nomenclature

{ }	Function
H	Head.
q	Flow rate
$Hy.HP$	Hydraulic Horsepower
P	Pressure (Psia)
ΔP	Pressure increment (psi)
λ_g	Volumetric free gas fraction
ρ	Density
BHP	Brake Horsepower, HP
g	Gravitational constant, 32.17 ft/sec ²
k	Ratio of specific heats (1.4 for air as an ideal gas)
M_g	Gas mass flow rate, lb _m /min
M	Air molecular weight, 28.97 lb _m /lb-mol
R	Ideal gas constant, 10.7316 psi-ft ³ /(lb-mol °R)
SG	Specific gravity, dimensionless
T	Temperature, °F
D	Pressure increment Degradation

Subscripts/ Superscripts

tp	Two-phase
sp	Single-Phase
$stage$	Across each stage
m	Mixture
w	Water
l	Liquid
g	Gas
d	Dimensionless
max	Maximum
SC	Standard Conditions (14.7 psia, 60 °F)
hom	Homogeneous

References

1. Cirilo, R.: *Air-Water Flow Through Electric Submersible Pumps*, MS Thesis. The University of Tulsa, Oklahoma (1998).
2. Lea, J.F. and Bearden, J.L.: "Effect of Gaseous Fluids on Submersible Pump Performance," paper SPE 9218 published in the *JPT* (December 1982) pp 2922-2930
3. Pessoa, R., Machado, M., Robles, J., Escalante, S. and Henry, J.: "Tapered Pump Experimental Tests with Light and Heavy Oil in PDVSA INTEVEP Field Laboratory," SPE-ESP Workshop (April 1999).
4. Pessoa, R. "Experimental Investigation of Two-Phase Flow Performance Of Electrical Submersible Pump Stages," MS Thesis, The University of Tulsa (2000).

5. Romero, M.: *An Evaluation of an Electric Submersible Pumping System for High GOR Wells*, MS Thesis, The University of Tulsa, Tulsa, Oklahoma (1999).
6. Sachdeva, R.: *Two-Phase Flow Through Electric Submersible Pumps*, MS Thesis. The University of Tulsa, Oklahoma (November 1998).
7. Sachdeva, R., Doty, D.R., and Schmidt, Z.: "Performance of Axial Electric Submersible Pumps in Gassy Well", paper SPE 24328 presented at the SPE Rocky Mountain Regional Meeting held in Casper, Wyoming. (May 18-21, 1992).
8. Turpin, J.L., Lea, J.F. and Bearden, J.L.: "Gas-Liquid Flow Through Centrifugal Pumps-Correlation of Data," 3rd Int'l Pump Symposium, Texas A&M University (May 1986).
9. Sun, D., Pessoa, R. and Prado, M.: "Single-Phase Model for Radial ESP's Performance" TUALP ABM. Tulsa, OK November 17, 2000.
10. Pessoa, R, Sun, D. and Prado, M.: "State of the Art: Experimental Work on ESP Performance under Two-Phase Flow Conditions", TUALP ABM. Tulsa, OK November 17, 2000
11. API Practice for Electrical Submersible Pump Testing," second edition, august 1997
12. Kallas, P and Way K," an electrical submersible pumping system for high GOR wells," SPE Electrical submersible pump workshop, April 26-28, 1995
13. Wilson, D.G et al.: " Analytical Models and Experimental Studies of Centrifugal Pump Performance in TEO Flow,' MIT Research project 493, NP -677, (1979), prepared for EPRI
14. Wilson, B.L.: " Gas handling centrifugal Pumps," SPE electrical submersible pump Workshop, (1998).

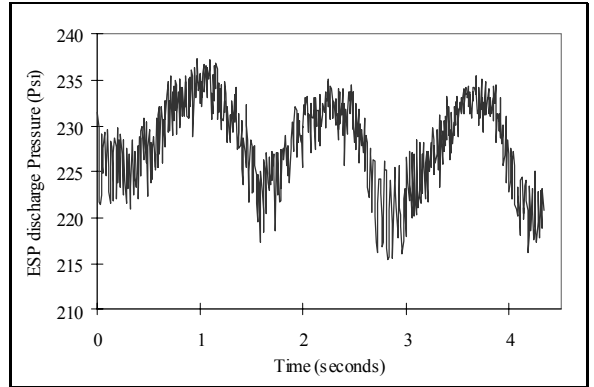


Figure 2: Discharge Pressure Fluctuation During Surging

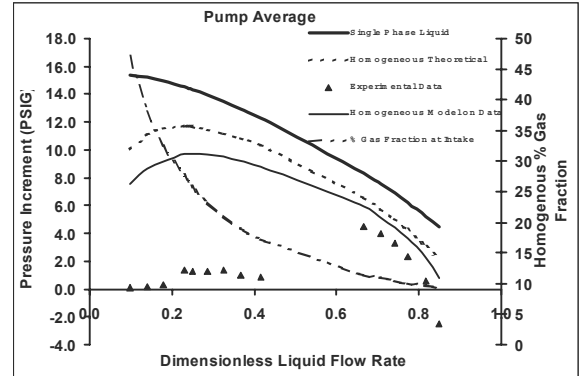


Figure3: Comparison of Homogeneous Models with Actual Performance for Average Pump Performance at Gas 30000 SCFD-Pressure 100 psig



Figure 4: ESP test bench after modifications

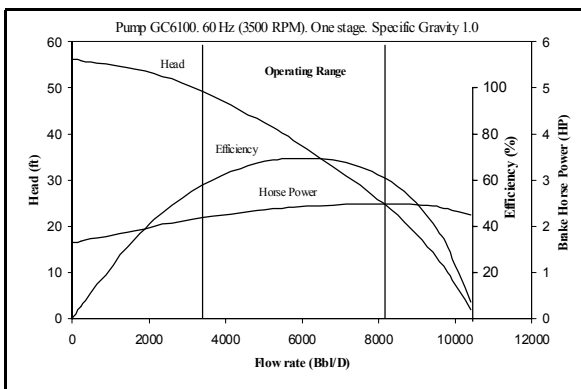


Figure 1: Manufacturer Pump Performance Curves

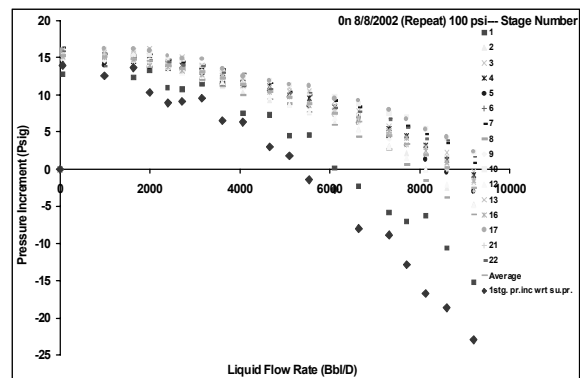


Figure 5: Single Phase Performance at 100 Psi

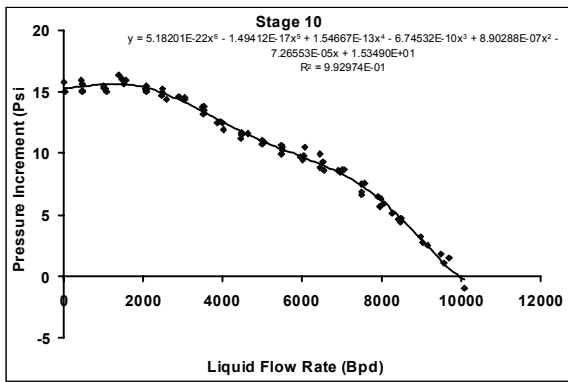


Figure 6: The average performance of 10th stage

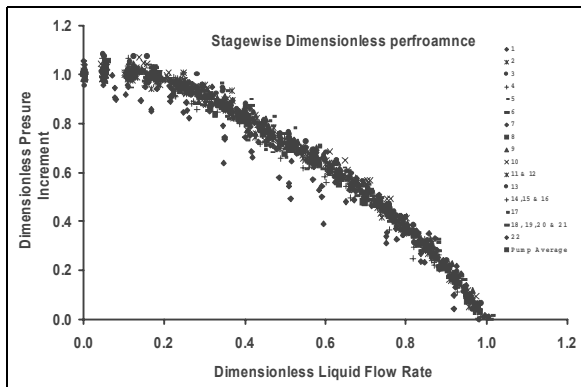


Figure 7: Stage-wise Dimensionless Performance showing except for the first stage all are falling in narrow range.

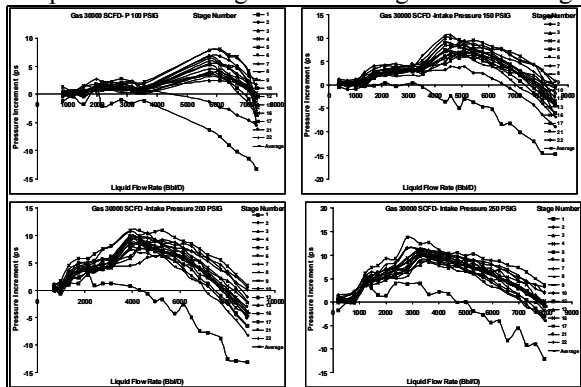


Figure 8: Stage-wise performance at different intake pressure for a gas flow rate of 30000 SCFD

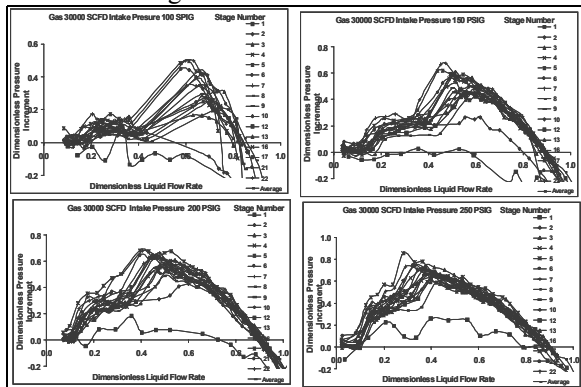


Figure 9: Dimensionless performance of stages at different intake pressures for a gas flow rate of 30000 SCfd

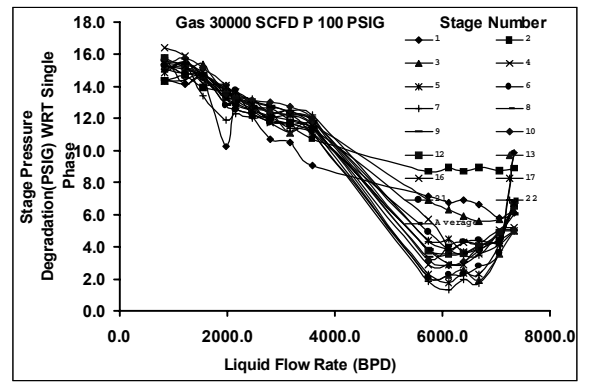


Figure 10: Stage-wise Performance Degradation With Respect To Single-Phase At Gas 30000 SCFD-Pressure 100 psig

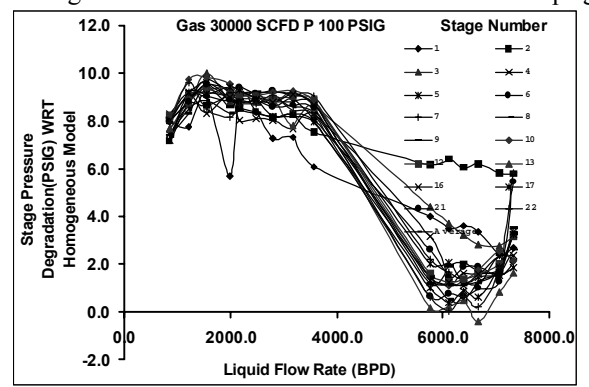


Figure 11: Stage-wise Performance Degradation With Respect To Homogeneous Model At 30000 SCFD-100 psig

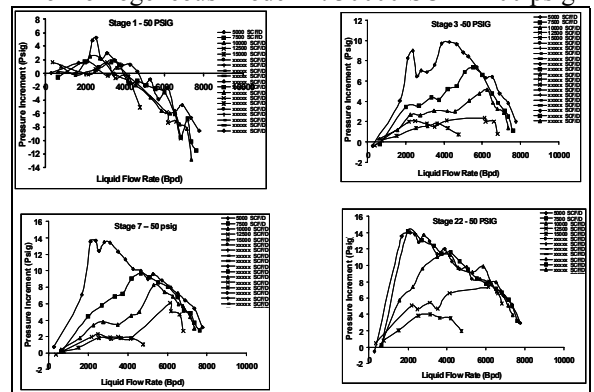


Figure 12: Effect of stage position at the pump intake pressure of 50 psig

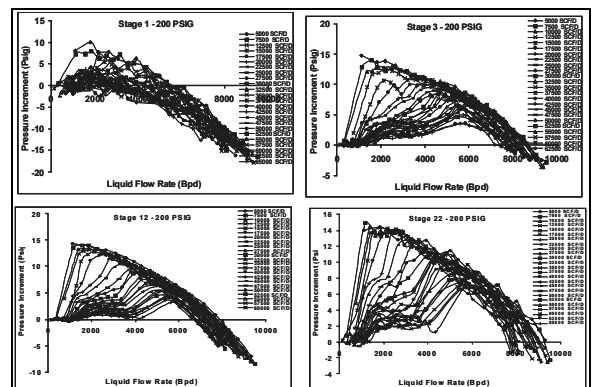


Figure 13: Effect of stage position at the pump intake pressure of 200 psig

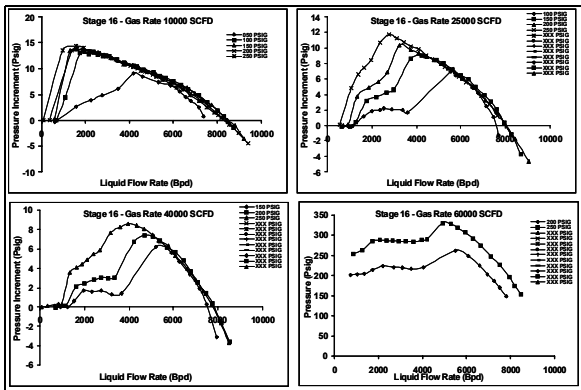


Figure 14: Example for effect of Pump intake pressure on 16th stage performance.

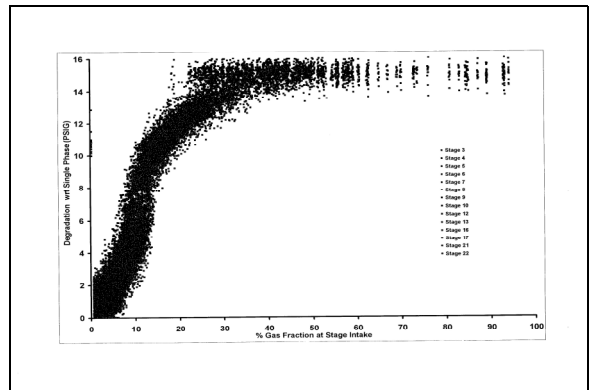


Figure 18: Pressure Increment Degradation with respect to single-phase Vs stage intake gas fraction

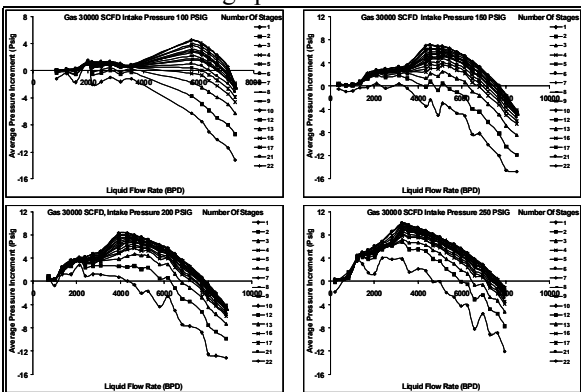


Figure 15: Effect on average stage performance with the number of stages

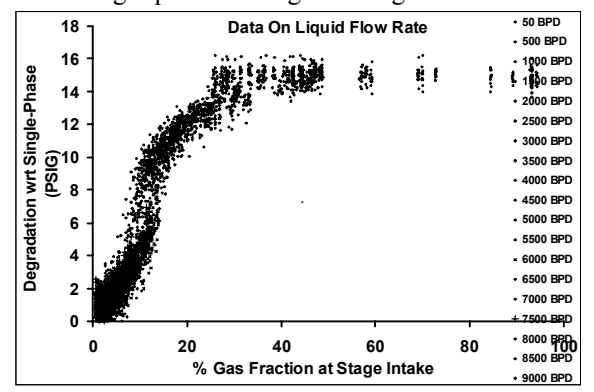


Figure 19: Pressure degradation with respect to single-phase Vs stage intake gas fraction sorted on liquid flow rate

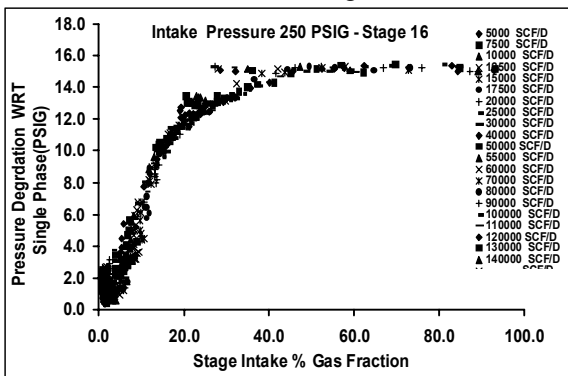


Figure 16: Effect of Gas fraction at stage intake on performance degradation with respect to single-phase

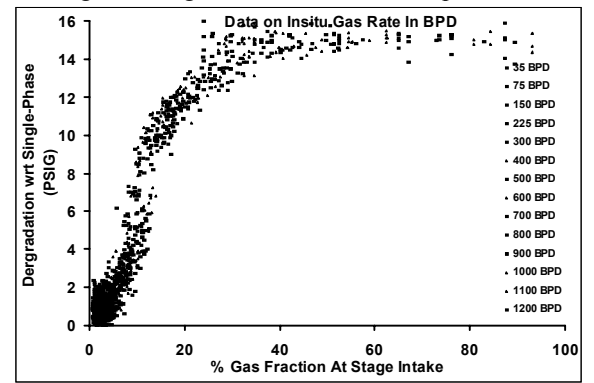


Figure 20: Pressure degradation with respect to single-phase Vs stage intake gas fraction sorted on Insitu gas flow rate

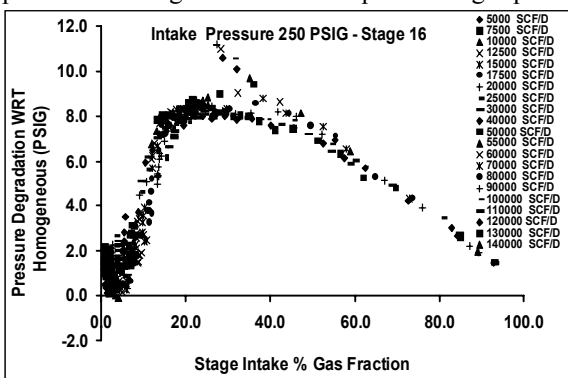


Figure 17: Effect of Gas fraction at stage intake on performance degradation with respect to Homogeneous model

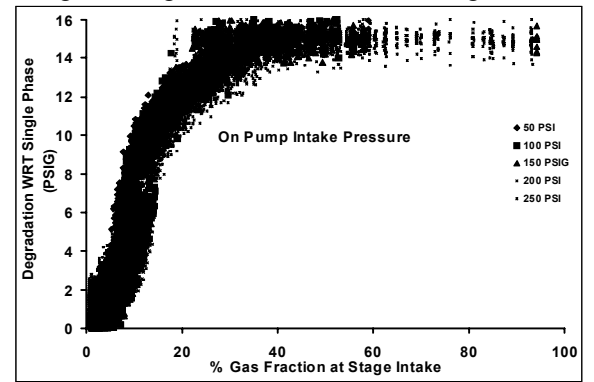


Figure 21: Pressure degradation with respect to single-phase Vs stage intake gas fraction sorted on Pump Intake Pressure

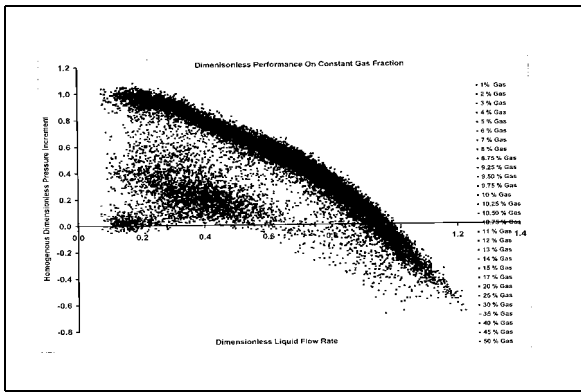


Figure 22: Homogeneous dimensionless Pressure increment Vs Dimension liquid flow rate for different stage intake gas fraction

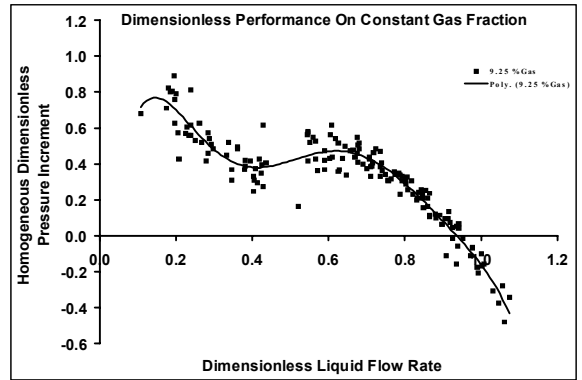


Figure 26: Homogeneous Dimensionless Pressure increment at 9.25 % gas fraction

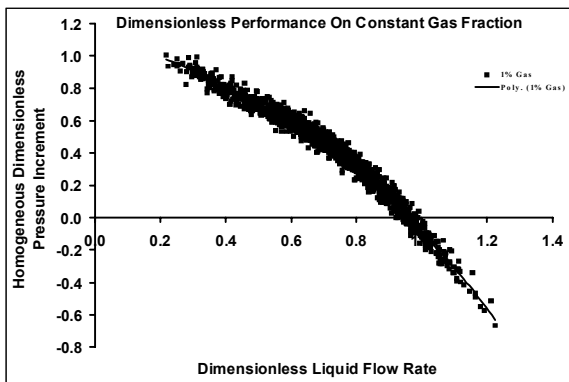


Figure 23: Homogeneous Dimensionless Pressure increment at 1% gas fraction

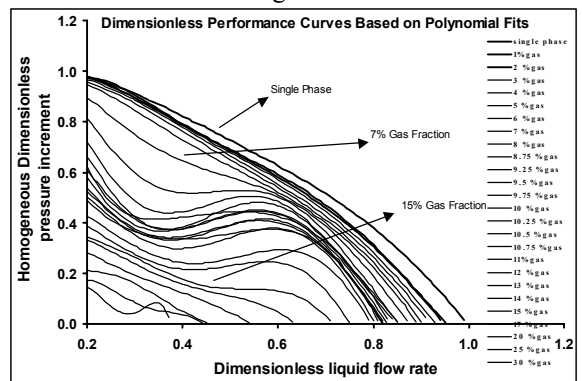


Figure 27: Homogeneous Dimensionless Pressure increment at different gas fraction based on sixth degree polynomial fit

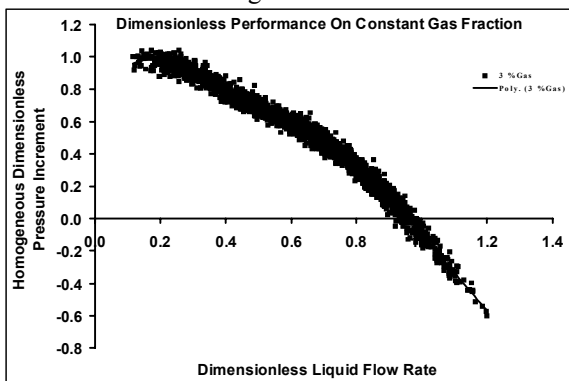


Figure 24: Homogeneous Dimensionless Pressure increment at 3 % gas fraction

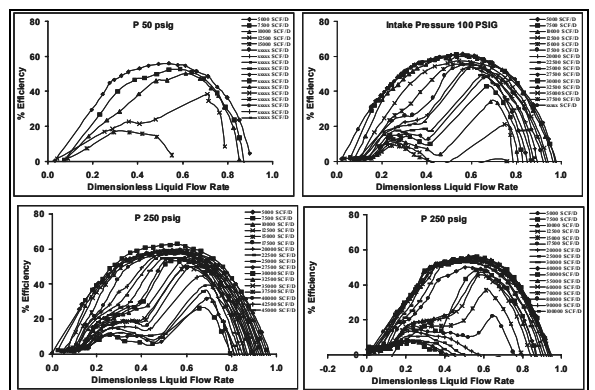


Figure 28: Efficiency curves based on adiabatic gas compression

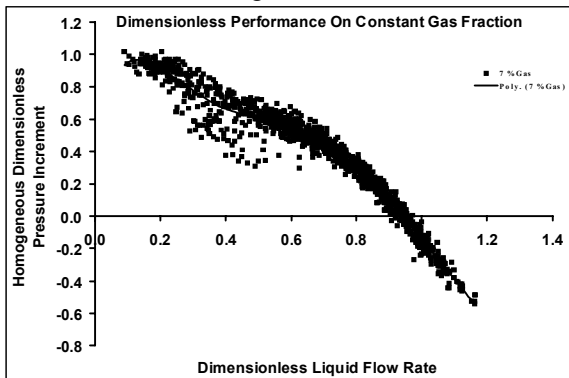


Figure 25: Homogeneous Dimensionless Pressure increment at 7 % gas fraction

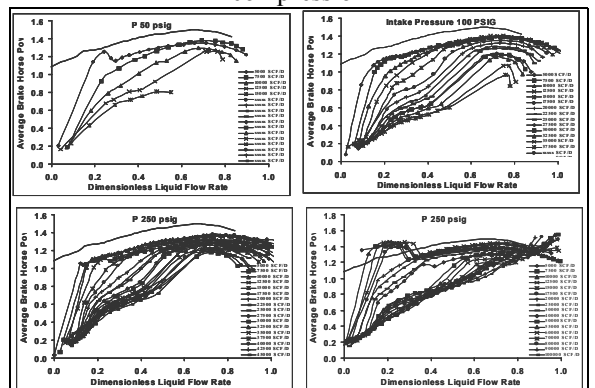


Figure 29: Plot showing average BHP consumption at different intake pressure